An integral method for the calculation of turbulent forced convection in a rotating cavity with radial outflow

John W. Chew
Theoretical Science Group, Rolls-Royce plc, Derby, UK

and Ruth H. Rogers
Thermo-Fluid Mechanics Research Centre, School of Engineering and Applied Sciences, University of Sussex, Brighton, UK

Received 28 February 1987 and accepted for publication 21 September 1987

The work of Owen, Pincombe, and Rogers[3] makes use of integral momentum techniques to investigate the flow of an isothermal fluid in a rotating cavity with an imposed radial throughflow. This paper extends the method to include the entraining boundary layer in the source region and to include an integral energy equation to predict the temperature in the core of the fluid when the discs of the cavity are heated. The effects of fluid property variations and frictional heating are also taken into account. The effect of various approximations are discussed, and the way in which the computed heat transfer depends on the mass flow coefficient, the rotational Reynolds number and the type of disc temperature distribution is found.

Keywords: heat transfer; integral method; rotating disc

Introduction

In the design of gas turbine engines estimates are required of the convective heat transfer to rotating compressor and turbine discs. This paper presents a technique for predicting the turbulent convective heat transfer from two corotating discs with a forced radial outflow of fluid between the discs. A model experiment is considered in which the two discs, each of radius b, are rotating with angular velocity Ω (see Figure1). The distance between the discs is s and each has a circular hole of radius a in the center. It is assumed that air at temperature T_I is blown uniformly into the cavity (that is, into the space between the discs) across the cylindrical surface $r=a$, and that the rate of mass flow through this surface is $\dot{m}$. The air leaves the cavity through the cylindrical surface $r=b$. The temperatures of the discs are specified as functions of the distance r from the axis.

The structure of the flow in isothermal conditions is well established from experimental and numerical studies (see, for example, Owen and Pincombe[1] and Chew, Owen, and Pincombe[2]); it is shown schematically in Figure 1. There is a source region ($a<r\leqslant r_e$) in which the incoming fluid is entrained into the boundary layers on the discs. For $r>r_e$, these boundary layers become nonentraining and bear a strong resemblance to Ekman layers: for this reason they will be referred to as *Ekman-type* layers. The fluid is redistributed from the Ekman-type layers into a sink layer near $r=b$, ready for exit from the cavity through a shroud at $r=b$. The region between the Ekman-type layers, the source region, and the sink layer is referred to as the core: the radial and axial components of velocity are zero in this region.

Integral momentum techniques were used by Owen, Pincombe, and Rogers[3] to predict the tangential component of velocity in the core and also the thickness of the Ekman-type layers on the discs, for an isothermal cavity; this paper will be referred to below as I. In the present contribution, the method is extended to include calculation of the entraining boundary layer; also an integral energy equation is incorporated to allow prediction of heat transfer. Some allowance for fluid property variations has also been made. The integral momentum method employed is an extension of that due to von Kármán[4] for the free disc (that is, a disc rotating in a quiescent infinite environment), and the method of calculating heat transfer is related to that of Dorfman[5] for the free disc.

The flow in a heated cavity is not as well understood as that for the isothermal case. Owen and Onur[6] have reported unsteady nonaxisymmetric flow in a cavity with one heated disc. However, the three different heat transfer regimes for radial outflow identified by Owen and Onur show qualitative agreement with numerical results for laminar flow in which buoyancy terms were neglected (Chew[7]). From theoretical considerations supported by numerical results (Chew[8]) it is expected that the flow structure in a heated cavity will be the same as for the isothermal case, provided that the temperature distributions are the same on each disc. When there is an axial temperature difference between the discs, buoyancy effects tend to transfer fluid between the two Ekman-type layers and the axial component of velocity is nonzero in the core. The results of a theoretical study of turbulent buoyancy-driven flow between two discs (Chew[9]) may be compared with the linear Ekman-layer solution given in I; this suggests that buoyancy effects are negligible when the nondimensional group $0.113(\Delta T/T_{ref})Re_\phi^{0.5}C_w^{-0.625}$ is small. Here ΔT is the temperature difference between the discs, T_{ref} is a reference temperature, Re_ϕ is a rotational Reynolds number, and C_w is a mass flow rate parameter (Re_ϕ and C_w are defined in Equation 2). This condition is satisfied in many cases of interest, and the transfer of fluid between the two Ekman-type layers will be neglected here. Further support for the validity of this assumption is provided by Long and Owen[10,11] and by Northrop and Owen[12], who compare experimental results with the present predictive method.

In the second section the basic integral equations are derived

under certain simplifying assumptions. Analytical solutions to the integral equations are possible in some cases, and these are presented in the third section. Numerical solutions of the equations are given in the fourth section, and the effects of some of the simplifying assumptions are investigated using these results. Finally, the main conclusions of this work are summarized in the fifth section. A detailed evaluation of the method against experimental results is presented by Northrop and Owen[12]; one of their figures is included in this paper for immediate comparison.

Derivation of the primitive integral equations

The notation is similar to that used in I, but, in view of the slight differences which are necessary in discussing the heated cavity, all quantities will be redefined here.

The axis of rotation of the discs is taken as the z-axis, and the disc surfaces are $z=0$ and $z=s$. It is assumed throughout that there is symmetry in the axial direction about the plane $z=\frac{1}{2}s$, and the subscript 0 is used to denote values on the disc at $z=0$. An overbar is used to indicate values outside the boundary layers on the discs, whether these are the entrainment layers of the source region or the Ekman-type layers bounding the core region. The subscript I is used for values appropriate to the incoming air, and these values will be used as reference values where necessary. On occasion, mean values (especially of density and viscosity) are used, and they are denoted by the subscript m: thus

$$\rho_m=\tfrac{1}{2}(\bar{\rho}+\rho_0), \qquad \mu_m=\tfrac{1}{2}(\bar{\mu}+\mu_0) \tag{1}$$

The local values of all quantities have no subscript except when they are independent of z within the boundary layer: then the

Notation

a	Inner radius of discs
b	Outer radius of discs
B_i, $i=1,13$	Coefficients in integral equations
c	Inlet swirl fraction
c_P	Specific heat at constant pressure
C_m	Moment coefficient, $2M/\rho_I\Omega^2b^5$
C_w	Mass flow rate coefficient, $\dot{m}/\mu_I$b
E	Eckert number, $\Omega^2r^2/2c_P(T_0-T_I)$
$f(\eta)$	Profile of radial component of velocity
$F(\mathrm{Pr})$	Factor in relationship between Nu*, Re, R_T
$g(\eta)$	Profile of tangential component of velocity
$G(x)$	Factor in approximate expression for Nu, Equation 48
$h(\eta, x)$	Profile of enthalpy
H	Enthalpy
I_i, $i=1,6$	Integrals involving $f(\eta)$, $g(\eta)$, and $h(\eta, x)$, Equations 17 and 41
J_i, $i=1,6$	Generalized form of the integrals I_i, Equations 61 to 66
k	Thermal conductivity
K	Factor in approximate expression for $\mathrm{Nu_{av}}$, Equation 56
K_n	Coefficient in expression for $\tau_{\phi,0}$
$\dot{m}$	Total mass flow rate into cavity
M	Moment on one disc
n	Reciprocal of exponent in power law for velocity profiles
Nu	Nusselt number for use with experimental comparisons, $rq_0/k_I(T_0-T_I)$
Nu*	Nusselt number used in Appendix A, $rq_0/k_I(T_0-\bar{T}-R\bar{v}^2/2c_P)$
p	Static pressure
P	$\bar{p}/\rho_I\Omega^2b^2$
P_n	Coefficient in expression for δ^*_{lin}
P'_n	Coefficient in expression for λ_0
Pr	Prandtl number
q	Heat transfer in axial direction
r	Radial coordinate
R	Recovery factor
R_T	Thermal Reynolds number, Equation 76
Re	Local Reynolds number, Equation 79
Re_ϕ	Rotational Reynolds number, $\rho_I\Omega b^2/\mu_I$
s	Distance between discs
T	Temperature
u	Radial component of velocity
$u_0(r)$	Scale factor for u
v	Tangential component of velocity referred to axes rotating with the cavity
V	$\bar{v}/\Omega r$
w	Axial component of velocity
x	r/b
z	Axial coordinate
α	$(3n+5)/2(n+1)$
β	Exponent in relationship between Nu*, Re, R_T
γ	Ratio of local mass flow rate through boundary layer to $\frac{1}{2}\dot{m}$
δ	$\rho_I\delta^*/\rho_I\delta^*_{lin}$
δ^*	Thickness of boundary layer
ΔT	Difference in temperature of the two discs
$\zeta(\mathrm{Pr})$	Correction factor for Nu when $T_0-T_I\propto r^2$, $\mathrm{Pr}\neq 1$
η	z/δ^*
θ	$(H_0-\bar{H})/H_0$
λ_0	Parameter in linear theory, Equation 27
μ	Dynamic viscosity
ξ	x^α/λ_0
ρ	Density
τ_r	Radial component of stress
τ_ϕ	Tangential component of stress
ϕ	Tangential coordinate angle
χ	General correction for Nusselt number when Reynolds analogy does not hold
Ψ	$\tau_{\phi,0}/(\tau_{\phi,0})_{lin}$
Ω	Angular speed of rotation of cavity

Subscripts

0	Value on disc (except for u_0, λ_0)
av	Average over disc face
b	Value when $r=b$
e	Value at transition from entrainment to Ekman-type layer
I	Value at inlet
l	Local value independent of z
lin	Value using linear theory with $\rho=\rho_I$, $\mu=\mu_I$, $\gamma=1$
m	Mean of value on disc and in core
n	Value for particular power law
r	Radial component
ref	Reference value (usually inlet value or when Reynolds analogy holds)
spec	Value when $T_0-T_I\propto r^2$, $\mathrm{Pr}\neq 1$
ϕ	Tangential component

Overbar indicates value in core

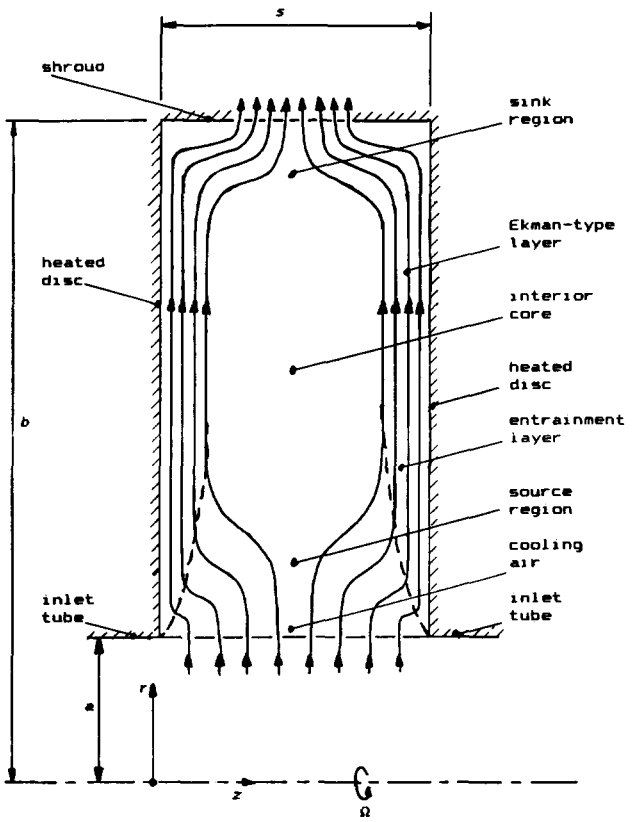

Figure 1 Schematic diagram of the cavity

subscript l is used, and the local value of the mass flow rate through the boundary layer is denoted by $\dot{m}_l$.

The density of the fluid is ρ, its viscosity is μ, its temperature is T, and its total enthalpy H; the pressure is p and the velocity has components (u, v, w) in the radial, tangential, and axial directions, referred to a frame of reference rotating with the discs at an angular velocity Ω about the z-axis. Cylindrical polar coordinates (r, ϕ, z) are used, with the same rotating frame of reference, and it is assumed that all the variables are independent of ϕ.

It is convenient at this point to define certain nondimensional parameters. A mass flow parameter C_w and a rotational Reynolds number Re_ϕ are given by

$$C_w=\frac{\dot{m}}{\mu_1 b}, \qquad \mathrm{Re}_\phi=\frac{\rho_1\Omega b^2}{\mu_1} \tag{2}$$

The nondimensional dependent variables of the problem are

$$V=\frac{\bar{v}}{\Omega r}, \quad \delta=\frac{\rho_l}{\rho_1}\frac{\delta^*}{\delta^*_{\mathrm{lin}}}, \quad \gamma=\frac{2\dot{m}_l}{\dot{m}}$$
$$\theta=\frac{H_0-\bar{H}}{H_0}, \quad P=\frac{\bar{p}}{\rho_1\Omega^2 b^2} \tag{3}$$

where ρ_l may be taken as $\bar{\rho}$, ρ_0, or ρ_m; δ^*_{lin} is the value of δ^* obtained by neglecting the nonlinear terms in the isothermal equations (with uniform temperature T_1) and taking $\gamma=1$; $\dot{m}_l$ is the local mass flow rate through one boundary layer (so that, when all the incoming fluid is entrained equally into the two boundary layers, $\gamma=1$). Nondimensional axial and radial coordinates are defined as

$$\eta=\frac{z}{\delta^*}, \qquad x=\frac{r}{b} \tag{4}$$

In the following two subsections, integral momentum and energy equations will be derived for the boundary layer on the disc $z=0$; they will be obtained by integrating the boundary layer equations between $z=0$ and $z=\delta^*$, where δ^* is the boundary layer thickness. Outside the boundary layer in the source region, it will be assumed that the tangential velocity can be calculated as for a free isothermal vortex (so that $V+1\propto x^{-2}$) and that the total enthalpy, $\bar{H}$ is uniform. It is also assumed, when considering the boundary layer flow, that the radial component of velocity in $\delta^*<z<s-\delta^*$ is negligibly small (compared to the speed of the disc). Thus, if $V_1=-1$, the integral equations for the entraining boundary layer reduce to those for a free disc. (Similarity of the flow and heat transfer in this layer to that of the free disc has previously been noted by Chew, Owen, and Pincombe[2] and Chew[7] in numerical studies of laminar flow.) No account has been taken of the sink layer in this study; the influence of the layer is confined to a small region near $r=b$, and so it is not expected to affect severely the heat transfer from the disc.

The momentum equations

The derivation of the integral momentum equations is similar to that in I, although some modification to allow for fluid property variations is required. In this section, it will be assumed that property variations across the boundary layer are negligible; ρ and μ will be replaced by ρ_l and μ_l throughout the equations, where ρ_l and μ_l are functions of r but not of z. The influence of density variations across the boundary layer will be discussed further in the fourth section in the subsection entitled "The effect of variable density within the boundary layer."

With the usual boundary layer assumptions, the continuity and momentum equations, in dimensional form, are

$$\frac{1}{r}\frac{\partial}{\partial r}(\rho_l u r)+\frac{\partial}{\partial z}(\rho_l w)=0 \tag{5}$$

$$\frac{1}{r}\frac{\partial}{\partial r}(\rho_l u^2 r)+\frac{\partial}{\partial z}(\rho_l u w)-\frac{\rho_l}{r}(v+\Omega r)^2+\frac{\partial p}{\partial r}=\frac{\partial \tau_r}{\partial z} \tag{6}$$

$$\frac{1}{r^2}\frac{\partial}{\partial r}(\rho_l u v r^2)+\frac{\partial}{\partial z}(\rho_l v w)+2\Omega\rho_l u=\frac{\partial \tau_\phi}{\partial z} \tag{7}$$

$$\frac{\partial p}{\partial z}=0 \tag{8}$$

Using Equation 8 and the radial momentum equation outside the boundary layers, one can easily show that

$$\frac{\mathrm{d}p}{\mathrm{d}r}=\frac{\rho_l}{r}(\bar{v}+\Omega r)^2 \tag{9}$$

Here, as is consistent with the model described above, the contribution of the nonzero radial velocity in the source region to the pressure gradient has been neglected.

The following forms are assumed for the velocity profiles in the boundary layer:

$$u=u_0 f(\eta), \qquad v=\bar{v}g(\eta) \tag{10}$$

where u_0 is a function of r only, f and g have to be specified in such a way that

$$f(0)=g(0)=0 \tag{11}$$

and

$$f(\eta)=0, \quad g(\eta)=1 \qquad \text{when } \eta\geqslant 1 \tag{12}$$

Further, it is assumed that

$$\frac{f(\eta)}{g(\eta)}\to 1 \qquad \text{as } \eta\to 0 \tag{13}$$

(Note that g is defined in a slightly different way from the form used in I: there, the second of Equations 10 was $v=\bar{v}[1-g(\eta)]$.)

Using Equations 9 and 10 and integrating Equations 5 to 7 gives

$$\rho_l \bar{w} = -\frac{I_1}{r}\frac{\mathrm{d}}{\mathrm{d}r}(r\rho_l u_0 \delta^*) \tag{14}$$

$$\frac{I_2}{r}\frac{\mathrm{d}}{\mathrm{d}r}(r\rho_l u_0^2 \delta^*) + \frac{\rho_l}{r}\delta^* \bar{v}^2 I_5 + 2\rho_l \delta^* \bar{v}\Omega I_4 = -\tau_{r,0} \tag{15}$$

$$\frac{I_3}{r^2}\frac{\mathrm{d}}{\mathrm{d}r}(r^2 \rho_l u_0 \bar{v}\delta^*) + \rho_l \bar{v}\bar{w} + 2I_1 \rho_l u_0 \Omega \delta^* = -\tau_{\phi,0} \tag{16}$$

where

$$I_1 = \int_0^1 f(\eta)\,\mathrm{d}\eta, \quad I_2 = \int_0^1 f^2(\eta)\,\mathrm{d}\eta, \quad I_3 = \int_0^1 f(\eta)g(\eta)\,\mathrm{d}\eta$$

$$I_4 = 1 - \int_0^1 g(\eta)\,\mathrm{d}\eta, \quad I_5 = 1 - \int_0^1 g^2(\eta)\,\mathrm{d}\eta \tag{17}$$

It is assumed that, near the disc, the ratio of the radial and transverse components of stress is equal to the ratio of the radial and transverse components of the fluid velocity relative to the rotating disc (see, for example, von Kármán[4]). Hence, from relations 10 and 13,

$$\tau_{r,0} = \frac{u_0}{\bar{v}}\tau_{\phi,0} \tag{18}$$

It is convenient to express Equations 15 and 16 in nondimensional form using Equations 2–4, together with the solution to the isothermal "linear" equations; in these the inertial terms in Equations 15 and 16 are negligible compared with the Coriolis terms, the radial mass flow is divided equally between the two boundary layers (so that $\gamma = 1$) and the density is assumed constant with $\rho = \rho_l$ throughout the boundary layer. (This solution has already been referred to in the definition of δ.)

The equations then become

$$\frac{x}{\delta}\frac{\mathrm{d}\delta}{\mathrm{d}x} = B_1 \frac{x}{\gamma}\frac{\mathrm{d}\gamma}{\mathrm{d}x} + B_2 + B_3 \frac{\Psi}{\gamma V} + (B_4 V^2 + B_5 V + B_6)\left(\frac{\delta}{\gamma V_{\mathrm{lin}}}\right)^2 \tag{19}$$

and

$$\frac{x}{V}\frac{\mathrm{d}V}{\mathrm{d}x} = B_7 \frac{x}{\gamma}\frac{\mathrm{d}\gamma}{\mathrm{d}x} + B_8 + B_9 \frac{1}{V} + B_{10}\frac{\Psi}{\gamma V} \tag{20}$$

where

$$\Psi = \frac{\tau_{\phi,0}}{(\tau_{\phi,0})_{\mathrm{lin}}} \tag{21}$$

and the coefficients B_k are given in the first column of Table 1. In this form, the equations may be used for any choice of profiles for the velocity and temperature.

In this paper, computations for turbulent flow are presented with velocity profiles which are generalizations of those used by von Kármán[4]; they are the same as those used in I, and are given by

$$f(\eta) = \eta^{1/n}(1-\eta), \qquad g(\eta) = \eta^{1/n} \tag{22}$$

where n is usually taken as 7. It is assumed, as in I and by analogy with von Kármán's solution, that

$$\tau_{\phi,0} = K_n^2 \rho_l \left(\frac{\mu_l}{\rho_l \delta^*}\right)^{2\alpha-3} \bar{v}(u_0^2 + \bar{v}^2)^{2-\alpha} \tag{23}$$

where

$$\alpha = \frac{3n+5}{2(n+1)} \tag{24}$$

Table 1 The coefficients B_k in the integral equations

k	Approximate equations: General	Approximate equations: $n=\frac{1}{7}$	Full equations
1	2	2	$2+\left(\frac{J_2'(\theta)}{J_2(\theta)} - \frac{2J_1'(\theta)}{J_1(\theta)}\right)B_{11}$
2	$1-\alpha$*	−0.625*	$1-\alpha+\left(\frac{J_2'(\theta)}{J_2(\theta)} - \frac{2J_1'(\theta)}{J_1(\theta)}\right)B_{12}\frac{x}{T_0}\frac{\mathrm{d}T_0}{\mathrm{d}x}$*
3	$-\frac{2I_1}{I_2}$	−3.94	$-\frac{2J_1(\theta)}{J_2(\theta)} + \left(\frac{J_2'(\theta)}{J_2(\theta)} - \frac{2J_1'(\theta)}{J_1(\theta)}\right)B_{13}\theta$
4	$\frac{I_1 I_5}{I_2 I_4}$	3.50	$\frac{J_1^2(\theta)J_5(\theta)}{J_1(0)J_4(0)J_2(\theta)}$
5	$\frac{2I_1}{I_2}$	3.94	$\frac{2J_1^2(\theta)J_4(\theta)}{J_1(0)J_4(0)J_2(\theta)}$
6	0	0	$\frac{J_1^2(\theta)J_0(\theta)}{J_1(0)J_4(0)J_2(\theta)}$
7	$\frac{I_1}{I_3}-1$	0.2	$\frac{J_1(\theta)}{J_3} - 1 + \left(\frac{J_1'(\theta)}{J_1(\theta)} - \frac{J_3'(\theta)}{J_3(\theta)}\right)B_{11}$
8	−2	−2	$-2+\left(\frac{J_1'(\theta)}{J_1(\theta)} - \frac{J_3'(\theta)}{J_3(\theta)}\right)B_{12}\frac{x}{T_0}\frac{\mathrm{d}T_0}{\mathrm{d}x}$
9	$-\frac{2I_1}{I_3}$	−2.4	$-\frac{2J_1(\theta)}{J_3(\theta)}$
10	$\frac{2I_1}{I_3}$	2.4	$\frac{2J_1(\theta)}{J_3(\theta)} + \left(\frac{J_1'(\theta)}{J_1(\theta)} - \frac{J_3'(\theta)}{J\theta)}\right)B_{13}\theta$
11	$\frac{I_1}{I_6}-1$	0.2**	$\left[\frac{J_1(\theta)}{J_1'(\theta)}\left(1-(1-\theta)\frac{J_1(\theta)}{J_1(0)}\right)\right]\frac{1}{\theta}$**
12	$\frac{I_1}{I_6}$	1.2**	$\frac{J_1(\theta)}{J_1'(\theta)} + \theta$**
13	$\frac{2I_1}{I_6}$	2.4**	$\frac{2J_1^2(\theta)}{J_1(0)J_1'(\theta)}$**

* $\alpha = -\frac{x}{V_{\mathrm{lin}}}\frac{\mathrm{d}V_{\mathrm{lin}}}{\mathrm{d}x}$.

** Assuming $h(\eta, x) = g(\eta)$.

so that $\alpha = 1.625$ when $n = 7$. It is shown in I that, with these assumptions,

$$\frac{\delta^*_{\mathrm{lin}}}{b} = P_n |C_w|^{2-\alpha} \mathrm{Re}_\phi^{-\frac{1}{2}} x^{\alpha-2} \tag{25}$$

and

$$V_{\mathrm{lin}} = -\lambda_0 x^{-\alpha} \tag{26}$$

where

$$\lambda_0 = \mathrm{sgn}(C_w) P_n' |C_w|^{\alpha-1} \mathrm{Re}_\phi^{-\frac{1}{2}} \tag{27}$$

The constants K_n, P_n, and P_n' are tabulated for $n = 5, 6, 7, 8, 9$ in Table 4 of I; in particular (for the case used for the computations in this paper),

$$K_7^2 = 0.0225, \quad P_7 = 0.159, \quad P_7' = 2.22 \tag{28}$$

Using these expressions in Equation 21, one can show that

$$\Psi = \frac{\rho_l}{\rho_I}\left(\frac{\mu_l}{\mu_I}\right)^{2\alpha-3} \frac{V|\gamma|^{4-2\alpha}}{V_{\mathrm{lin}}\delta}\left(\frac{I_4}{I_1+I_4}\right)^{2-\alpha}\left[1+\frac{I_1}{I_4}\left(\frac{V\delta}{\gamma V_{\mathrm{lin}}}\right)^2\right]^{2-\alpha} \tag{29}$$

The energy equation

As in the last section, property variations across the boundary layer are neglected. It will also be assumed that the thickness of the thermal boundary layer is the same as that of the velocity boundary layer. In the source region, this follows the method used by Dorfman[5] for the free disc. In the core outside the Ekman-type layers, it is assumed that $\bar{u}=0$ and, from symmetry, $\bar{w}=0$: hence there is no convection in this region. If radial diffusion of heat is negligible compared with axial diffusion, it follows that, in the steady state, all the temperature variation is within the momentum boundary layer. In reality, some radial diffusion will occur within the core, but this effect is expected to be small in cases of practical interest.

The appropriate form of the energy equation is

$$\frac{1}{r}\frac{\partial}{\partial r}(\rho urH)+\frac{\partial}{\partial z}(\rho wH)=-\frac{\partial}{\partial z}[q-u\tau_r-(v+\Omega r)\tau_\phi] \tag{30}$$

where the total enthalpy H is defined as

$$H=c_PT+\tfrac{1}{2}[u^2+(v+\Omega r)^2+w^2] \tag{31}$$

q is the heat flux in the axial direction and c_P denotes the specific heat of the fluid at constant pressure. The total enthalpy profile is assumed to have the form

$$H=H_0[1-\theta h(\eta,r)] \tag{32}$$

Two methods have been used for estimating h and the surface heat flux q_0; they are described here, and a comparison between them is made in the subsection "The effect of varying Prandtl number." The simplest method, motivated by the Reynolds analogy (see the Appendix), is to assume that

$$h(\eta)=g(\eta) \tag{33}$$

and

$$\frac{q_0}{c_P}=\zeta\left(T_0-\bar{T}-\frac{R\bar{v}^2}{2c_P}\right)\frac{\tau_{\phi,0}}{\bar{v}} \tag{34}$$

where ζ and R are functions of the Prandtl number, Pr. When dissipation effects are neglected, the work of Dorfman[5] can be generalized to give the expression

$$\zeta=\left[1+5\left(\mathrm{Pr}-1+\log_e\left[\frac{5\mathrm{Pr}+1}{6}\right]\right)\left(\frac{\tau_{\phi,0}}{\rho_1V^2\Omega^2r^2}\right)^{1/2}\right]^{-1} \tag{35}$$

(This is identical with the result of von Kármán[13] for a flat plate.) A commonly used approximation is

$$\zeta=\mathrm{Pr}^{-0.4} \tag{36}$$

For the flow over a flat plate, Rotta[14] gives an expression for R which, when modified for a rotating disc, may be written as

$$R=1+94.75\mathrm{Pr}^{-0.4}(\mathrm{Pr}-1)\frac{\tau_{\phi,0}}{\rho_1V^2\Omega^2r^2} \tag{37}$$

where the coefficient $94.75\mathrm{Pr}^{-0.4}$ is obtained (as an approximation) by interpolation from Table 23.1 given by Schlichting.[15] Many authors, according to Schlichting, take

$$R=\mathrm{Pr}^{1/3} \tag{38}$$

for turbulent flow. The effect of using the approximations 36 and 38 instead of the more elaborate expressions 35 and 37 is discussed in the subsection "The effect of the temperature distribution on the disc."

The second method makes some allowance for the variation of the function $h(\eta,r)$ with Prandtl number and the temperature distribution on the disc. It is discussed in detail in the Appendix.

The expression for q_0 becomes

$$\frac{q_0}{c_P}=\chi\left(T_0-\bar{T}-\frac{R\bar{v}^2}{2c_P}\right)\frac{\tau_{\phi,0}}{\bar{v}} \tag{39}$$

where χ is a function of Prandtl number and now also depends on the disc temperature distribution. The form used for χ is discussed in the Appendix and is given by

$$\chi=\left(\frac{I_1-I_6}{I_1-I_3}\right)^{3-2\alpha}\zeta^{2(\alpha-1)} \tag{40}$$

where

$$I_6=\int_0^1 h(\eta,x)f(\eta)\,\mathrm{d}\eta \tag{41}$$

No explicit expression for h is used, and the integral I_6 is determined as described below.

Integrating Equation 30 across the boundary layer, using Equations 31, 32, and 39, and introducing the nondimensional variables, we get

$$x\frac{\mathrm{d}\theta}{\mathrm{d}x}=B_{11}\frac{x}{\gamma}\frac{\mathrm{d}\gamma}{\mathrm{d}x}\theta+(B_{12}-\theta)\frac{x}{H_0}\frac{\mathrm{d}H_0}{\mathrm{d}x}-\frac{x}{I_6}\frac{\mathrm{d}I_6}{\mathrm{d}x}\theta+B_{13}\frac{\Psi}{\gamma}\left[\frac{\chi\theta}{V}+\frac{\Omega^2b^2x^2}{H_0}(\tfrac{1}{2}\chi V(1-R)+\chi-1)\right] \tag{42}$$

where the coefficients B_k are given in Table 1.

For the first method, χ is replaced by ζ, $I_6=I_3$ and $\mathrm{d}I_6/\mathrm{d}x=0$. Equation 42 is not used in the entrainment layer, but is used in the Ekman-type layer to determine θ.

In the second method, Equation 42 is used in the entrainment layer (where θ is known) to determine I_6. For the Ekman-type layers, the equation is used to determine θ and it assumed (see the appendix) that I_6 is constant.

Analytical solutions

In certain cases, analytical solutions of the integral equations are available. These give a useful insight into the numerical solutions for more general conditions which will be discussed in the next section; in addition, they give approximations which may be used for quick engineering calculations.

The free disc

The integral momentum equations for a disc rotating in an infinite quiescent environment were first derived and solved by von Kármán.[4] The entrained mass flow, the boundary layer thickness, and the shear stress on the disc obtained from von Kármán's solution (in which $n=7$ and fluid properties are assumed constant) are given by

$$\frac{\dot{m}_i}{\mu_i r}=0.219(\mathrm{Re}_\phi x^2)^{0.8} \tag{43}$$

$$\frac{\delta^*}{r}=0.525(\mathrm{Re}_\phi x^2)^{-0.2} \tag{44}$$

$$\frac{\tau_{\phi,0}}{\rho_i\Omega^2r^2}=0.0267(\mathrm{Re}_\phi x^2)^{-0.2} \tag{45}$$

Von Kármán's solution has been extended to include heat transfer by Dorfman[5] using the Reynolds analogy between shear stress and heat flux. This solution is valid when $\mathrm{Pr}=1$, $T_0-T_1\propto r^2$, where T_1 is now the fluid temperature at large distances from the disc and frictional dissipation is negligible. Introducing a Nusselt number $\mathrm{Nu}=rq_0/k_1(T_0-T_1)$, this

solution gives

$$\mathrm{Nu}=0.0267(\mathrm{Re}_\phi x^2)^{0.8} \tag{46}$$

Dorfman also considered the effect of varying Prandtl number and disc temperature distribution. His final expression for the Nusselt number may be written

$$\mathrm{Nu}=0.0188(\mathrm{Re}_\phi x^2)^{0.8}\mathrm{Pr}^{0.6}G(x) \tag{47}$$

where

$$G(x)=x^{0.65}(T_0-T_\mathrm{I})^{0.25}\left[\int_0^x (T_0-T_\mathrm{I})^{1.25}x^{2.25}\,\mathrm{d}x\right]^{-0.2} \tag{48}$$

Dorfman claims that his solution gives agreement with measurements from an isothermal disc.

Owen[16] has shown that the Reynolds analogy can be extended to include frictional heating. This effect should be included when the Eckert number

$$E=\frac{\Omega^2 r^2}{2c_P(T_0-T_\mathrm{I})} \tag{49}$$

is not negligibly small. For $\mathrm{Pr}=1$ and $T_0-T_\mathrm{I}\propto r^2$, Equation 46 still holds if the factor $(1-E)$ is inserted on the right side of the equation. Unfortunately, Dorfman's analysis is not easily extended to include frictional heating and, in the absence of any definitive experimental evidence it is not clear whether Equation 47, or a modified form of it, is valid when frictional effects are significant.

Ekman-layer flow

A solution of the integral momentum equations was found in I for the case in which the advective terms are negligible and the fluid properties are uniform; this is referred to above as the "linear solution." It is analogous to the linear Ekman-layer solution in laminar flow and is relevant to the constant-mass-flow boundary layer that develops once all the supplied fluid has been entrained into the boundary layers on the disc. It was shown in I that, although $|V|$ is assumed small in the derivation of the linear solution, Equation 26 is in surprisingly good agreement with measurements and with numerical solutions of the full equations for $|V|$ up to 0.67.

The linear solutions for V and δ^* are given by Equations 25 and 26. The corresponding solution for $\tau_{\phi,0}$, the shear stress on the disc, is

$$\frac{(\tau_{\phi,0})_\mathrm{lin}}{\rho_\mathrm{I}\Omega^2 b^2}=-\frac{1}{2\pi x}C_w\mathrm{Re}_\phi^{-1} \tag{50}$$

Putting $V=V_\mathrm{lin}$ in Equation 20, a higher-order estimate of $\tau_{\phi,0}$ may be deduced. For $n=7$, this gives

$$\frac{\tau_{\phi,0}}{\rho_\mathrm{I}\Omega^2 b^2}=-\frac{1}{2\pi x}C_w\mathrm{Re}_\phi^{-1}(1-0.156\lambda_0 x^{-1.625}) \tag{51}$$

This equation has a similar range of validity, as an approximation to the solution of the full integral equations, to that of V_lin.

When $\mathrm{Pr}=1$ and $T_0-T_\mathrm{I}\propto r^2$, the Reynolds analogy, as for the free disc, gives the heat transfer from the disc. Details of this analogy are given by Chew.[17] The resulting expression for the local Nusselt number, based on the disc-to-inlet temperature difference (T_0-T_I), is

$$\mathrm{Nu}=\frac{C_w}{2\pi x}(1-E_b)(1-0.156\lambda_0 x^{-1.625}) \tag{52}$$

where E_b is the value of E evaluated at $r=b$. The range of validity of Equation 52 is similar to that for Equation 51 for the shear stress.

For more general conditions the Reynolds analogy does not apply, and an explicit expression for an approximate value of Nu is not at present available. Work in progress will, it is hoped, remedy this situation.

Average quantities on the cavity disc

Although the Ekman-layer solutions are not valid over the inner part of the disc, an estimate of the moment coefficient for the whole disc may be obtained by considering the angular-momentum balance for the cavity and assuming that the linear Ekman solution holds at $r=b$. The resulting expressions for the moment coefficient C_m (where $C_m=2M/\rho_\mathrm{I}\Omega^2 b^5$, where M is the moment on one face of the disc) is

$$C_m=C_w\mathrm{Re}_\phi^{-1}\left[1-0.833\lambda_0-c\left(\frac{a}{b}\right)^2\right] \tag{53}$$

where the tangential velocity of the fluid entering the cavity in a stationary frame of reference is $c\Omega a$.

From an energy balance equation for the cavity, and assuming the Ekman-layer solution at $r=b$, an expression for the average Nusselt number, Nu_av, for the whole disc face may be deduced: this is defined as

$$\mathrm{Nu}_\mathrm{av}=\frac{q_\mathrm{av}b}{k_\mathrm{I}(T_{0,\mathrm{av}}-T_\mathrm{I})} \tag{54}$$

where q_av and $T_{0,\mathrm{av}}$, respectively, are the radially weighted average heat flux and disc temperature over the disc face. When $\mathrm{Pr}=1$ and $T_0-T_\mathrm{ref}\propto r^2$, Equation 54 becomes

$$\mathrm{Nu}_\mathrm{av}=K\frac{C_w}{2\pi}\frac{b^2}{b^2-a^2}\frac{T_{0,\mathrm{b}}-T_\mathrm{I}}{T_{0,\mathrm{av}}-T_\mathrm{I}} \tag{55}$$

where

$$K=1-E_b-0.833\lambda_0\left(\frac{T_{0,\mathrm{b}}-T_\mathrm{ref}}{T_{0,\mathrm{b}}-T_\mathrm{I}}-E_b\right)+c(2-c)E_b\left(\frac{a}{b}\right)^2 \tag{56}$$

The relationship (if any) between T_ref and T_I will depend on conditions at the inlet. When $\mathrm{Pr}\neq 1$, it may be assumed that, to a good approximation,

$$\mathrm{Nu}_\mathrm{av}=K\,\mathrm{Pr}\frac{C_w}{2\pi}\frac{b^2}{b^2-a^2}\frac{T_{0,\mathrm{b}}-T_\mathrm{I}}{T_{0,\mathrm{av}}-T_\mathrm{I}} \tag{57}$$

For more general conditions, when the Reynolds analogy does not hold, a good approximation is given by

$$\mathrm{Nu}_\mathrm{av}=\frac{\mathrm{Pr}C_w}{2\pi}\frac{b^2}{b^2-a^2}\frac{T_{0,\mathrm{b}}-T_\mathrm{I}}{T_{0,\mathrm{av}}-T_\mathrm{I}}\left[1-E_b+c(2-c)E_b\left(\frac{a}{b}\right)^2\right] \tag{58}$$

to the lowest order in the small quantities V and θ.

When C_w is large and Re_ϕ is small, the source region extends throughout the whole cavity. In this case, there are no Ekman-type layers on the discs and it may be assumed that the value of Nu_av given by Dorfman[5] for the free disc is appropriate. In this case,

$$\mathrm{Nu}_\mathrm{av}=0.0470[G(1)]^4\,\mathrm{Pr}\,\zeta(\mathrm{Pr})\frac{T_{0,\mathrm{b}}-T_\mathrm{I}}{T_{0,\mathrm{av}}-T_\mathrm{I}}(\mathrm{Re}_\phi x^2)^{0.8} \tag{59}$$

Numerical solutions

The integral momentum equations 19 and 20 and the integral energy equation 42 have been solved numerically using a variable-step Gear method. The computations were started at $x=a/b$, which was assumed to be in the entrainment layer. The model described in I was used for this layer, so $V=-1$ (a special

case for the free vortex), $\bar{H}=H_1$, and γ is unknown. The starting values used for the computations were $\delta=10^{-4}$, $\gamma=4\times10^{-7}$, and $I_6=I_3$; it was found that the solutions were insensitive to starting values of δ and γ for smaller values than this. The computation was continued with increasing x until γ had increased to the value unity. For values of x greater than this, the integral equations were used to find δ, V, and θ as functions of x in the region where the Ekman-type layer is present. Here it was assumed that $d\gamma/dx=0$, and I_6 was obtained either by putting $I_6=I_3$ or by putting $dI_6/dx=0$. The starting values for this part of the computation were found by assuming the dependent variables to be continuous at the transition from the entrainment layer to the Ekman-type layer.

In the ensuing discussion, x will be retained as the dependent variable; for computational purposes it was convenient to use instead the variable $\xi=x^a/\lambda_0$, where λ_0 is defined in Equation 27. Clearly, for the linear solution discussed above, $V_{lin}=-1/\xi$.

Most computations were carried out with $a=42.75$ mm, $b=427.5$ mm, and $T_I=30°C$. Values of $C_w=1400$ and 14,000, of $Re_\phi=3\times10^6$, and of $Pr=1$ and 0.71 were used. Three temperature distributions on the disc were considered; these were $T_0=T_I+70°x^2$, $T_I+45°$, and $T_I+14°/x$. The local Nusselt number

$$Nu=\frac{rq_0}{k_I(T_0-T_I)} \tag{60}$$

was computed and, with two exceptions, all the graphs show Nu as a function of x; in the other cases, the value of Nu_{av} is shown as a function of Re_ϕ for various values of C_w and various distributions of T_0.

The effect of variable density within the boundary layer ($Pr=1$)

In the derivation given above of the integral equations, it was assumed that the density variation across the boundary layer is negligible. The validity of this assumption is now investigated. When the density is not assumed independent of z, integrals of the form

$$J_0(\theta)=\frac{1}{1-\theta}-\int_0^1\frac{1}{1-\theta h(\eta)}d\eta \tag{61}$$

$$J_1(\theta)=\int_0^1\frac{f(\eta)}{1-\theta h(\eta)}d\eta \tag{62}$$

$$J_2(\theta)=\int_0^1\frac{f^2(\eta)}{1-\theta h(\eta)}d\eta \tag{63}$$

$$J_3(\theta)=\int_0^1\frac{f(\eta)g(\eta)}{1-\theta h(\eta)}d\eta \tag{64}$$

$$J_4(\theta)=\frac{1}{1-\theta}-\int_0^1\frac{g(\eta)}{1-\theta h(\eta)}d\eta \tag{65}$$

and

$$J_5(\theta)=\frac{1}{1-\theta}-\int_0^1\frac{g^2(\eta)}{1-\theta h(\eta)}d\eta \tag{66}$$

arise instead of the integrals I_k defined in Equation 17. ($J_0(0)=0$ and $J_k(0)=I_k$ for $k=1$ to 5.) Equations 19 and 20 are still valid, but the coefficients B_k are now those given in the last column of Table 1.

As discussed earlier, when $Pr=1$ and $T_0-T_I\propto r^2$ it may be assumed that $h=g$. Figure 2 shows comparisons between solutions for these conditions using both the full equations and the primitive equations. It can be seen that the difference between the two solutions is very small, in spite of the fact that the values of B_k vary considerably in the two methods. The computation using the correction takes about 10 times as long as that for the primitive equations. Considering these results and the uncertainties involved in applying the correction in more general conditions, inclusion of this correction for prediction of Nusselt numbers is not thought to be worthwhile.

The effect of viscous dissipation and compressive work ($Pr=1$)

Viscous dissipation will be significant when the Eckert number is not negligible. This parameter also governs the significance of the compressive work done on the air in the Ekman-type layers as it is transported through the radial pressure gradient.

To isolate these effects, a comparison of solutions was obtained using the full integral energy equation 42 and an integral energy equation in which viscous dissipation and compressive work were neglected. The latter equation may be obtained by replacing H by T in Equations 42 and 43 and by dropping the term with the factor Ω^2b^2 from Equation 42. For small rotational speeds, the difference between the solutions is negligible, but, as shown in Figure 3, at $Re_\phi=3\times10^6$, there are significant systematic differences between the two sets of results. For the results shown in the figure, the Eckert number E defined in Equation 49 has the value 0.08 when $r=b$.

The effect of varying the Prandtl number

As described above, the factors R and ζ are used to take account of the effect of the Prandtl number. Numerical experiments were carried out to determine the effect of using the approximations 36 and 38 for these parameters rather than Equations 35 and 37 for air. Figure 4 shows comparisons between the solutions, with $Pr=0.71$ and $T_0-T_I\propto r^2$, using the two sets of equations. It is clear that use of the approximate form causes little systematic

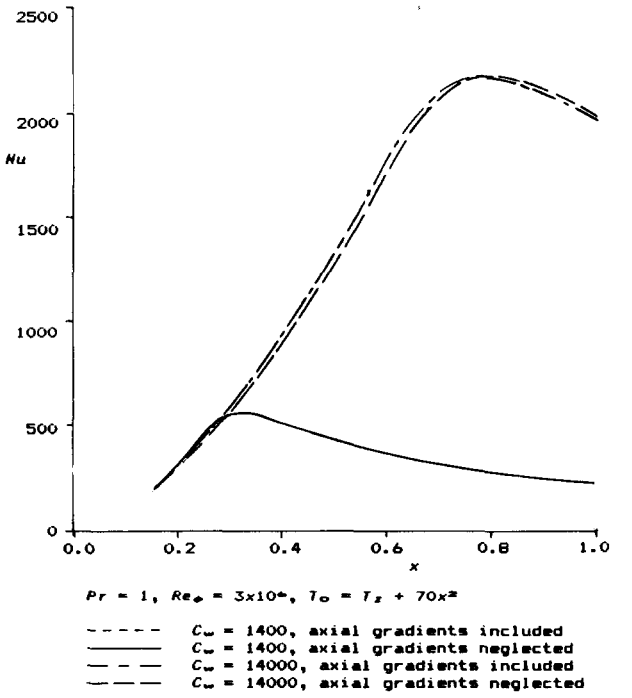

Figure 2 The effect of neglecting axial density gradients in the boundary layers

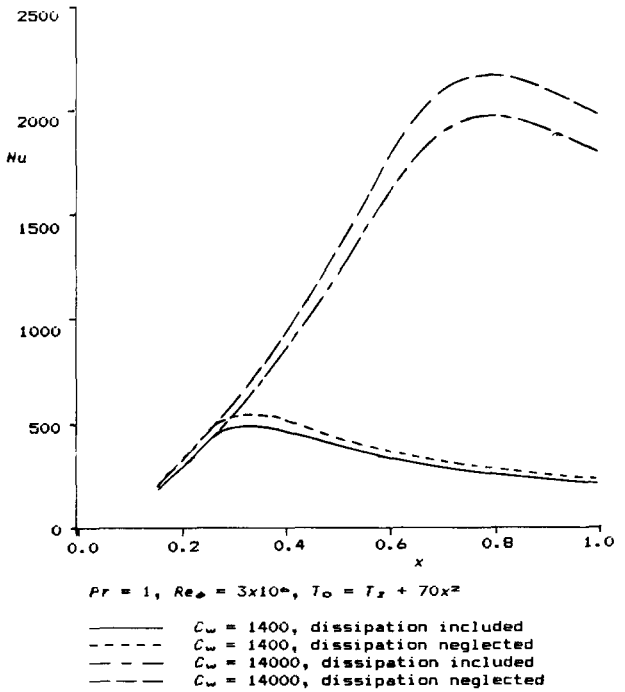

Figure 3 The effect of neglecting viscous dissipation

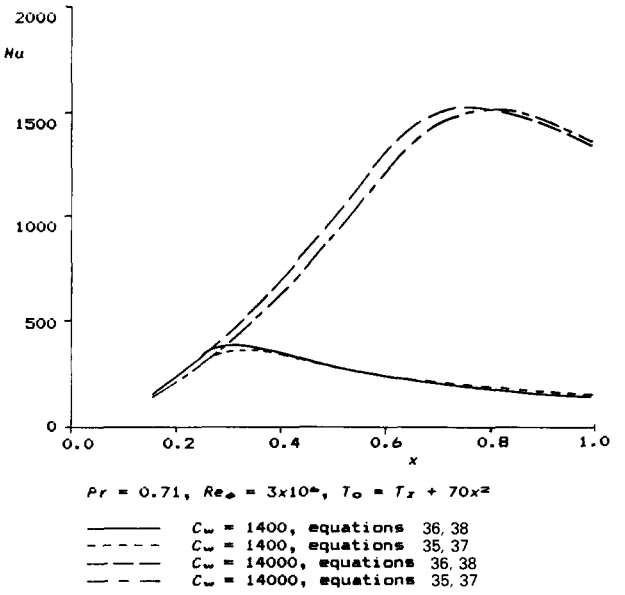

Figure 4 The effect of using approximate formulae for the functions R and ζ

error and reduces computational time. It is suggested, therefore, that Equations 36 and 38 should be used for R and χ.

The effect of the temperature distribution on the disc (Pr=0.71)

Nusselt number predictions for three different temperature distributions are shown in Figure 5. Numerical results are given for both methods of estimating q_0 and I_6 described above; the integral energy equation for method 1 (in which $I_6 = I_3$) being obtained by replacing χ by ζ in Equation 42. As is to be expected, the numerical results are indistinguishable when $T_0 = T_1 + 70x^2$, but there is a noticeable difference for other temperature distributions. It should be noticed, however, that both methods give maximum values of Nu at approximately the same value of x, and the same applies to zero values of Nu. Thus the correction has the effect of requiring a multiplicative factor on the value of Nu; this is hardly surprising in view of the nature of the assumption made by the use of Equation 39.

Whether the use of Equation 39 and the assumption that I_6 is constant in the Ekman-type layer (and continuous with the value in the entrainment layer) is superior to the use of Equations 33 and 34 (where it is assumed that $I_6 = I_3$) can be determined only by comparison with experiment. Some support for using the more complicated method is supplied by Dorfman[5] who showed agreement between theory and the measurements by Cobb and Saunders[18] of heat transfer from an isothermal disc rotating in air when dissipative effects are neglected. There is, however, some evidence that the second method may fail (due to excess stiffness) when there are large disc temperature gradients: in such cases, the first method may still be used.

The average Nusselt number

Figure 6 shows predictions of the variation of Nu_{av} with Re_ϕ for two values of C_w and for increasing, constant, and decreasing disc temperature distributions; the value of I_6 was computed using the more complicated method described above. The fall-off for large values of Re_ϕ and the negative values of Nu_{av} are due to the effects of frictional and compressive work, as discussed in the second subsection; the sharpness of the fall-off is remarkable. Clearly the mean Nusselt number is strongly dependent on the disc temperature distribution, on C_w, and on Re_ϕ. The dependency on Re_ϕ could be reduced somewhat by using an adiabatic disc temperature rather than the disc temperature itself in the definition of Nu_{av}. However, this requires a

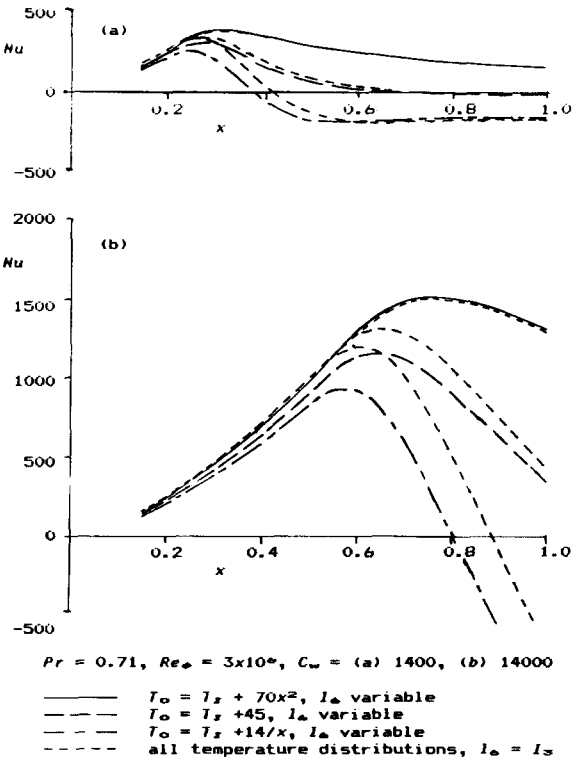

Figure 5 The effect of different disc temperature distributions

knowledge of the core velocity $\bar{v}$, and this is not generally available in heat transfer experiments.

Comparisons between the numerical results for Nu_{av} and the approximate analytical solutions given in the third section are shown in Figure 7. For $C_w = 1400$, Ekman-layer theory is appropriate; good agreement between the numerical results and Equation 57 for the quadratic disc temperature distribution or Equation 58 for other disc temperature distributions is found. The inadequacy of Equation 58 at low values of Re_ϕ when $C_w = 1400$ in Figure 7(a) is attributed to nonlinear effects which are neglected in the derivation of the equations. For $C_w = 14{,}000$, the free-disc solution given by Equation 59 is appropriate at lower values of Re_ϕ. At higher values of Re_ϕ, the numerical results and the Ekman-layer theory are converging. Clearly, judicious use of Equations 57 to 59 can give useful estimates of the mean heat transfer, but some caution must be exercised in the intermediate region where neither the free-disc theory nor the Ekman-layer theory is appropriate.

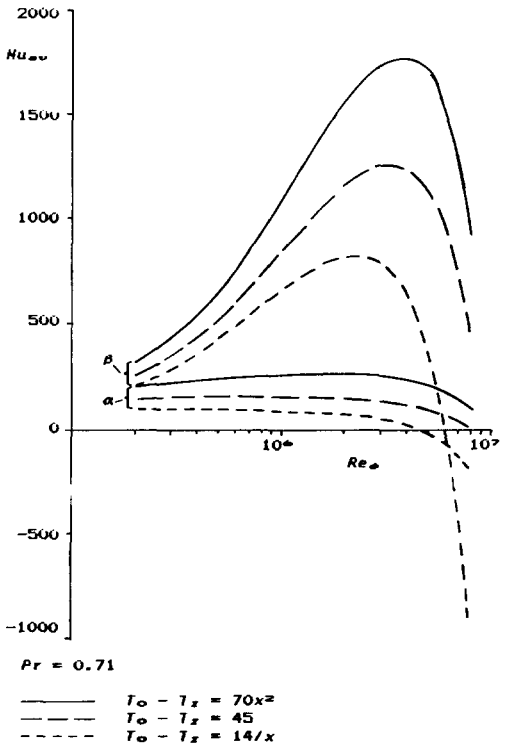

Figure 6 The average Nusselt number, Nu_{av}, as a function of Re_ϕ, using the integral solution: (α) $C_w = 1400$; (β) $C_w = 14{,}000$

Comparison with experimental data

Results from the present theory have been compared with heat transfer measurements by Long and Owen[10,11] and by Northrop and Owen.[12] The most reliable experimental data is probably that of Northrop and Owen, who obtained heat transfer measurements for a rotating cavity of aspect ratio $s/b = 0.138$ with essentially the same temperature distributions on the two discs; an example of their results is shown in Figure 8. The positive, constant, and negative profiles in this figure indicate disc temperature distributions in which T_0 was generally increasing, uniform, or decreasing with increasing r, respectively. In the experiments, air entered the cavity through a central hole $0 \leqslant x < 0.1$ in one of the discs, and it left the cavity through a series of holes in the outer cylindrical shroud. Estimates of the local Nusselt numbers were obtained both from heat fluxmeter measurements and from the numerical solution of the heat conduction problem for the disc, the boundary conditions being supplied by the measured temperatures on the disc. As illustrated by the results in Figure 8, agreement between the fluxmeter measurements, the conduction solution, and the present theory is mainly good. Not surprisingly, some departure of the theory from the measurements was noted at relatively high values of C_w and low values of Re_ϕ where the flow is no longer rotationally dominated.

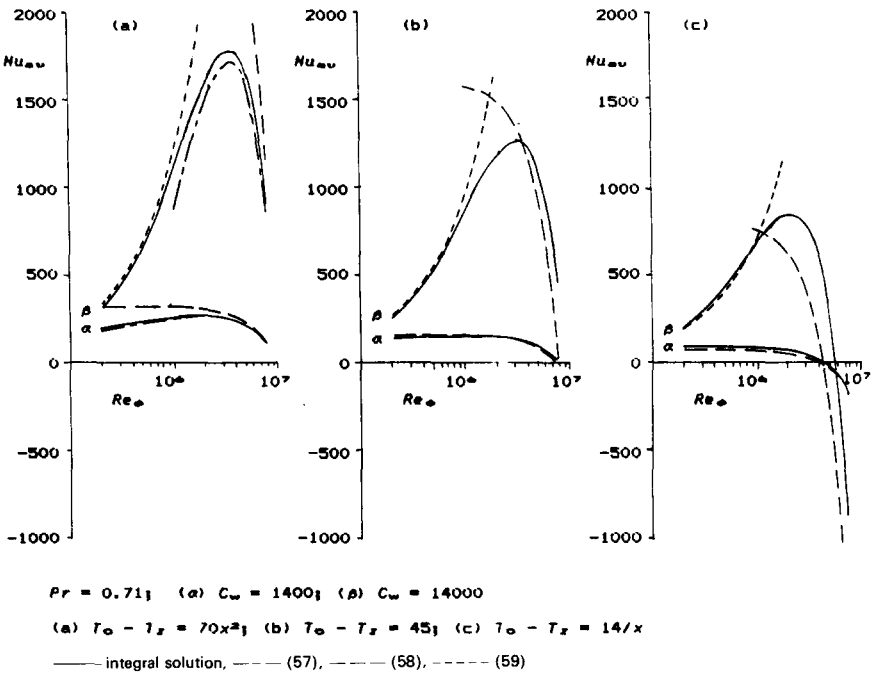

Figure 7 Comparison of the approximate solution for the average Nusselt number, Nu_{av}, with that using the integral solution

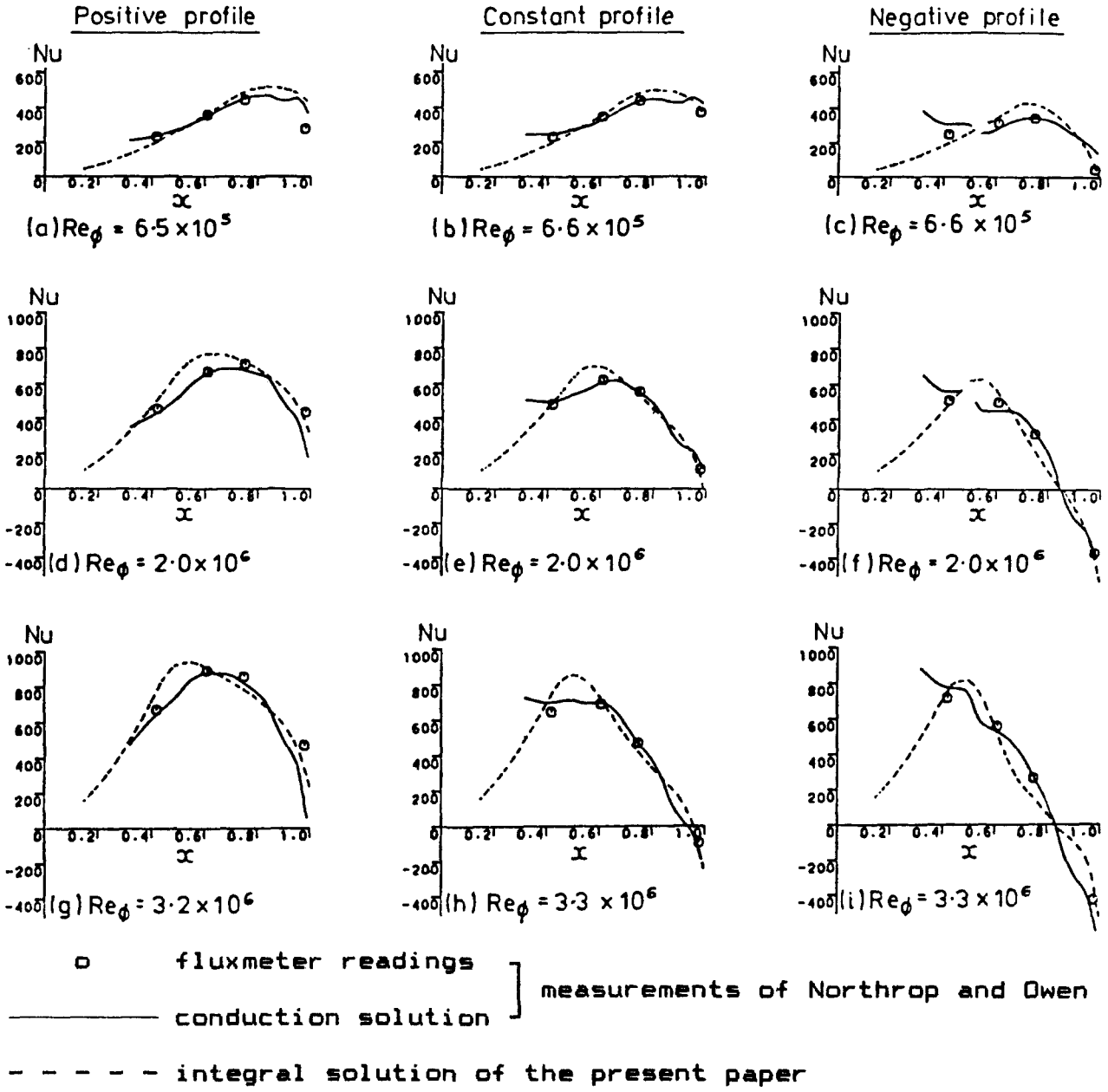

Figure 8 (Reproduced from Northrop and Owen[12]) The effect of temperature profiles and Re_ϕ on the variation of Nu with x: $C_w = 7000$; upstream disc

Conclusions

It has been shown that the integral technique used for the momentum equations in Ref. 3 can be usefully extended to find temperature distributions and, hence, heat transfer from the discs of a symmetrically heated rotating cavity. It is concluded that, in the momentum equations, it is sufficient to neglect the variation of density across the boundary layers on the disc; that it is necessary at high rotational Reynolds numbers to include the effect of dissipation in the energy equation; and that approximate expressions may be used for the factors introduced to allow for a Prandtl number not equal to unity. The results do show some sensitivity to the assumptions made to account for the effect of a nonquadratic disc temperature distribution on the Reynolds analogy, and some caution in applying the method to nonquadratic temperature distributions may be advisable.

Agreement between the present predictive method and measurements has been demonstrated by Long and Owen[10,11] and by Northrop and Owen.[12]

References

1 Owen, J. M. and Pincombe, J. R. Velocity measurements inside a rotating cylindrical cavity with a radial outflow of fluid. *J. Fluid Mech.*, 1980, **99**, 111

2 Chew, J. W., Owen, J. M., and Pincombe, J. R. Numerical predictions for laminar source-sink flow in a rotating cylindrical cavity. *J. Fluid Mech.*, 1984, **143**, 451

3 Owen, J. M., Pincombe, J. R., and Rogers, R. H. Source-sink flow inside a rotating cylindrical cavity. *J. Fluid Mech.*, 1985, **155**, 233

4 Kármán, Th. von. Über laminare und turbulente Reibung. *Z. Angew. Math. Mech.*, 1921, **1**, 233

5 Dorfman, L. A. *Hydrodynamic Resistance and the Heat Loss of Rotating Solids*. Oliver and Boyd, Edinburgh and London, 1963
6 Owen, J. M. and Onur, H. S. Convective heat transfer in a rotating cylindrical cavity. *ASME J. Engng Power*, 1983, **105**, 265
7 Chew, J. W. Computation of forced laminar convection in rotating cavities. *ASME J. Heat Transfer*, 1985, **107**, 277
8 Chew, J. W. Computation of convecting laminar flow in rotating cavities. *J. Fluid Mech.*, 1985, **153**, 339
9 Chew, J. W. Buoyancy-affected turbulent Ekman layer flow between rotating discs. Rolls-Royce report, 1983
10 Long, C. A. and Owen, J. M. Transient analysis of heat transfer in a rotating cavity with a radial outflow of fluid. Heat Transfer 1986: Proc. Eighth Int. Heat Transfer Conf., San Francisco, Vol. 3 (ed. Tien, C. L. *et al.*), Hemisphere, 1986, 1257
11 Long, C. A. and Owen, J. M. The effect of inlet conditions on heat transfer in a rotating cavity with a radial outflow of fluid. *J. Engng Power*, 1986, **108**, 145
12 Northrop, A. and Owen, J. M. Heat transfer measurements in rotating-disc systems. Part II: The rotating cavity with a radial outflow of cooling air. *Int. J. Heat Fluid Flow*, 1988, **9**, 27–36
13 Kármán, Th. von. The analogy between fluid friction and heat transfer. *Trans. ASME*, 1939, **61**, 705
14 Rotta, J. C. Temperaturverteilungen in der turbulenten Grenzschicht an der ebenen Platte. *Int. J. Heat Mass Transfer*, 1964, **7**, 215
15 Schlichting, H. *Boundary-Layer Theory*. McGraw-Hill, London, 1979
16 Owen, J. M. The Reynolds analogy applied to flow between a rotating and a stationary disc. *Int. J. Heat Mass Transfer*, 1971, **14**, 451
17 Chew, J. W. The effect of frictional heating and compressive work in rotating axisymmetric flow. *ASME J. Heat Transfer*, 1985, **107**, 984
18 Cobb, E. C. and Saunders, O. A. Heat transfer from a rotating disc. *Proc. Roy. Soc. A*, 1956, **236**, 343

Appendix: Formulae for the surface heat flux and the total enthalpy profile

The modified Reynolds analogy result

It is assumed that the relationship between the surface heat flux and the tangential component of the surface shear stress is of the form

$$\frac{q_0}{c_P}=\chi\left(T_0-\bar{T}-\frac{R\bar{v}^2}{2c_P}\right)\frac{\tau_{\phi,0}}{\bar{v}} \tag{67}$$

where χ depends on the Prandtl number and on the disc temperature distribution, and R depends on the Prandtl number only. The Nusselt number is defined as

$$\mathrm{Nu}^*=\frac{rq_0}{k_l(T_0-\bar{T}-R\bar{v}^2/2c_P)} \tag{68}$$

and it follows that

$$\mathrm{Nu}^*=\mathrm{Pr}\,\chi\frac{r\tau_{\phi,0}}{\mu_l\bar{v}} \tag{69}$$

In the special case for which $T_0-T_\mathrm{I}\propto r^2$, $\bar{v}_\mathrm{I}=-\Omega a$, and $\mathrm{Pr}=1$, Equation 67 must reduce to the Reynolds analogy (see Chew[17]). In this case, therefore, $\chi=1$ and $R=1$. This will be used as a "reference case," and the subscript ref will be used where appropriate. In the reference case, Equation 69 reduces to

$$\mathrm{Nu}^*_\mathrm{ref}=r\left(\frac{\tau_{\phi,0}}{\mu_l\bar{v}}\right)_\mathrm{ref} \tag{70}$$

and the total enthalpy profile is similar to that of the tangential component of velocity, so that

$$h_\mathrm{ref}(\eta,x)=g(\eta) \tag{71}$$

The effect of Prandtl number

It is useful to consider the special case of the free disc for which $T_0=T_{0,\mathrm{ref}}$, $\bar{v}=-\Omega r$, $\rho_l=\rho_\mathrm{I}$, $\mu_l=\mu_\mathrm{I}$, and $\bar{T}=T_\mathrm{I}$. The subscript spec is used to indicate this case, and it is assumed that χ_spec depends on Pr only. It is convenient to write $\zeta=\chi_\mathrm{spec}$, so Equations 67 and 69 become

$$\frac{q_{0,\mathrm{spec}}}{c_P}=\zeta\left(T_{0,\mathrm{ref}}-T_\mathrm{I}-\frac{R\Omega^2r^2}{2c_P}\right)\frac{(\tau_{\phi,0})_\mathrm{spec}}{\Omega r} \tag{72}$$

and

$$\mathrm{Nu}^*_\mathrm{spec}=-\mathrm{Pr}\,\zeta\frac{(\tau_{\phi,0})_\mathrm{spec}}{\Omega\mu_\mathrm{I}} \tag{73}$$

The values of ζ and R are taken to be those given in Equations 35 and 37 or, more usually, by the approximations 36 and 38.

When dissipation is neglected, Equation 42 for this case may be rearranged to give

$$\frac{\mathrm{d}}{\mathrm{d}x}\left[\frac{I_1-I_{6,\mathrm{spec}}}{\zeta}(\gamma T_0\theta)_\mathrm{spec}\right]=2I_1\frac{(\Psi T_0\theta)_\mathrm{spec}}{x} \tag{74}$$

For $\mathrm{Pr}=1$ it is assumed that $\zeta=1$ and $I_{6,\mathrm{spec}}=I_3$; consideration of the above equation (in which only $I_{6,\mathrm{spec}}$ and ζ depend on Pr) shows that

$$I_1-I_{6,\mathrm{spec}}=\zeta(I_1-I_3) \tag{75}$$

The effect of disc temperature distribution

It is possible to use a generalization of the method described by Dorfman[5] and to define a thermal Reynolds number

$$R_\mathrm{T}=\frac{\rho_l(u_0^2+\bar{v}^2)^{0.5}}{\mu_l}\int_0^{\delta^*}\frac{u(H-\bar{H})}{u_0(H_0-\bar{H})}\,\mathrm{d}z \tag{76}$$

In terms of the notation of this paper, Equation 76 gives

$$R_\mathrm{T}=\frac{\rho_l}{\mu_l}(u_0^2+\bar{v}^2)^{0.5}\delta^*(I_1-I_6) \tag{77}$$

It is assumed that, in general,

$$\mathrm{Nu}^*=F(\mathrm{Pr})\,\mathrm{Re}\,R_\mathrm{T}^\beta \tag{78}$$

where $F(\mathrm{Pr})$ is a universal function of Prandtl number, β is a universal constant, and Re is a local Reynolds number defined by

$$\mathrm{Re}=\rho_l(u_0^2+\bar{v}^2)^{0.5}\frac{r}{\mu_l} \tag{79}$$

(In general, R_T depends on Pr through the total enthalpy profile.)

Since β and $F(\mathrm{Pr})$ are universal functions, they may be determined by consideration of the special cases described in the first two sections. Using relations 23 for the shear stress in Equation 70, one can show that, under appropriate conditions, Equation 78 reduces to Equation 70 when

$$\beta=3-2\alpha \tag{80}$$

and

$$F(1)=\frac{K_n^2}{(I_1-I_3)^\beta} \tag{81}$$

Similarly, Equations 78 and 74 are consistent as long as

$$\frac{F(\mathrm{Pr})}{F(1)}=\left(\frac{I_1-I_3}{I_1-I_{6,\mathrm{spec}}}\right)^{\beta}\mathrm{Pr}\,\zeta \tag{82}$$

Substituting from Equations 75 and 81 gives

$$F(\mathrm{Pr})=\frac{K_n^2\,\mathrm{Pr}\,\zeta^{1-\beta}}{(I_1-I_3)^{\beta}} \tag{83}$$

Comparing the expressions for Nu in Equations 69 and 78 and using Equations 23, 77, 79, 80 and 83 gives

$$\chi=\left(\frac{I_1-I_6}{I_1-I_3}\right)^{3-2\alpha}\zeta^{2(\alpha-1)} \tag{84}$$

The entrainment layer in a rotating cavity

In this region H_0 and θ are known, and it is assumed that Equation 84 is valid. Then Equation 43 is used to determine I_6 and, hence, χ. Under the appropriate conditions, this method reproduces the solution given by Dorfman[5] and the Reynolds analogy results.

The Ekman-type layer in a rotating cavity

Here H_0 is known, but neither θ nor I_6 are known. Hence Equation 43 is inadequate to determine both unknowns, and an extra relationship is required. The simplest method is to assume that the enthalpy profile is similar to that of the tangential component of velocity; this gives $I_6=I_3$ and $\chi=\zeta$. It is evident that this is only an approximation and cannot be used unless the same assumption is made for the entrainment layer. Its justification is that results using integral methods are only weakly dependent on the form of the profiles chosen.

More sophisticated approaches have been tried: these give solutions which are significantly different from each other when theoretical profiles (other than quadratic ones) are used for the disc temperature, but which all agree with the available measurements to the level of experimental uncertainty. The method recommended here is to assume that I_6 is constant in the Ekman-type layer and to put $\mathrm{d}I_6/\mathrm{d}x=0$.